

Article

Optical Coherence Tomography Reveals Changes to Corneal Reflectivity and Thickness in Individuals with Tear Hyperosmolarity

Laura Adelaide Deinema¹, Algis Jonas Vingrys¹, Holly Rose Chinnery¹, and Laura Elizabeth Downie¹

¹ Department of Optometry and Vision Sciences, Faculty of Medicine, Dentistry & Health Sciences, The University of Melbourne, Parkville, Victoria, Australia 3010

Correspondence: Laura Downie, Department of Optometry and Vision Sciences, University of Melbourne, Parkville VIC, Australia 3010. e-mail: ldownie@unimelb.edu.au

Received: 26 December 2016

Accepted: 19 March 2017

Published: 22 May 2017

Keywords: tears; osmolarity; dry eye; cornea; hyperosmolarity

Citation: Deinema LA, Vingrys AJ, Chinnery HR, Downie LE. Optical coherence tomography reveals changes to corneal reflectivity and thickness in individuals with tear hyperosmolarity. *Trans Vis Sci Tech.* 2017;6(3):6. doi:10.1167/tvst.6.3.6 Copyright 2017 The Authors

Purpose: To investigate whether tear hyperosmolarity, a feature of dry eye disease (DED), affects central corneal thickness (CCT), corneal light reflectivity, and/or tear film reflectivity.

Methods: This prospective, cross-sectional study involved 48 participants (38 with hyperosmolar tears and 10 controls with normo-osmolar tears). Symptoms and signs of DED (tear osmolarity, sodium fluorescein tear break-up time, ocular surface staining, Schirmer test) were assessed. CCT, and the reflectivity of the cornea and the tear-epithelial interface were quantified relative to background noise using Fourier-domain optical coherence tomography (FD-OCT).

Results: CCT of eyes with severe tear hyperosmolarity, defined as eyes in the upper quartile of the hyperosmolar group, was less than control eyes (539.1 ± 7.4 vs. 583.1 ± 15.0 μm , $P = 0.02$) and eyes with less severe tear hyperosmolarity, defined as hyperosmolar eyes in the lower quartile (622.7 ± 5.8 μm , $P < 0.0001$). CCT showed a negative linear relationship with tear osmolarity for values above 316 mOsmol/L ($R^2 = 0.17$, $P = 0.01$). Central corneal reflectivity was lower in hyperosmolar eyes than normo-osmolar eyes (45.1 ± 0.3 vs. 48.1 ± 0.6 pixels, $P = 0.02$); the greatest relative difference was in the anterior stroma, where corneal reflectivity was $4.7 \pm 1.9\%$ less in hyperosmolar eyes ($P < 0.01$). Peak reflectivity of the tear-epithelial interface was $4.8\% \pm 3.5\%$ higher in the hyperosmolar group than the normo-osmolar tear group ($P = 0.04$).

Conclusion: Individuals with significant tear hyperosmolarity and clinical signs of symptoms of DED show reduced CCT and altered corneal reflectivity.

Translational Relevance: Anterior segment FD-OCT provides novel insight into corneal microstructural differences in individuals with DED.

Introduction

Dry eye disease (DED) is a complex, multifactorial condition that is associated with ocular surface damage and impaired visual performance.¹ In DED, lowered aqueous secretion and/or excessive tear evaporation increase the relative concentration of tear solutes. The resultant tear hyperosmolarity is proposed to trigger inflammatory pathways, which promote epithelial cell damage and tear film instability.¹⁻⁴

Given the potentially detrimental effects of tear hyperosmolarity on ocular surface integrity,^{5,6} a

negative impact upon corneal structure is predicted. Corneal transparency, which is imparted by the specific arrangement of collagen fibrils within the stroma to yield destructive light interference,⁷ relies upon the strict maintenance of corneal hydration. Corneal hydration is regulated predominantly by the corneal endothelium, but also relies upon a functional epithelial barrier.⁸ A disruption to corneal epithelial integrity could therefore influence corneal hydration, with secondary effects upon its transparency.

A link between tear osmolarity and changes to corneal structure has been described in an experimen-

tal animal model of tear hyperosmolarity. Desiccating stress, induced acutely by the application of a hypertonic agent to the rabbit cornea, reduces corneal thickness and increases corneal light backscatter.⁹ Furthermore, physiological diurnal fluctuations in tear osmolarity have been shown to correlate with changes in central corneal thickness (CCT) in human eyes, as quantified using high-resolution anterior segment optical coherence tomography (OCT).¹⁰ Preliminary evidence also suggests that individuals with clinical signs and symptoms of DED have reduced corneal thickness¹¹ and endothelial cell changes,¹² although the potential effect of tear osmolarity per se was not considered in these studies.

OCT enables noninvasive, in vivo cross-sectional imaging of the eye. High-resolution anterior segment OCT has been used to document longitudinal changes in corneal reflectivity subsequent to anterior ocular inflammation in rodent models.^{13–15} Our laboratory has demonstrated the utility of OCT for monitoring changes to corneal thickness and haze in a murine model of corneal inflammation.¹⁵ The application of OCT for measuring corneal pachymetry, described by Izatt and colleagues,¹⁶ was one of the earliest anterior eye applications of OCT.^{16,17} CCT measurements using OCT have been shown to be comparable to conventional ultrasound-based pachymetry techniques, being highly repeatable and reproducible with the additional advantage of being non-contact.^{17,18} OCT has been used to characterize changes during recovery to the structural and optical properties of the human cornea following surgical intervention.^{19–21} The technique has been applied to document alterations to corneal light reflectivity, as a measure of corneal haze, at the flap interface following laser-assisted in situ keratomileusis.²¹ In addition, OCT can quantify changes to tear film thickness in patients with DED.²²

Together, these studies provide rationale for examining the novel application of OCT to assess whether tear hyperosmolarity alters CCT, corneal and/or tear film reflectivity. This study tests the hypotheses that in individuals with DED, tear hyperosmolarity leads to alterations to corneal reflectivity, corneal thickness, and tear film reflectivity.

Methods

This project was conducted in accordance with the tenets of the Declaration of Helsinki and was approved by the University of Melbourne Human

Research Ethics Committee. All study participants provided written informed consent to participate.

Sample Size Calculation

An a priori target sample size of 49 participants, comprising of $n = 39$ with tear hyperosmolarity and $n = 10$ controls with normo-osmolar tears, using a 4:1 allocation ratio of cases:controls, returned 80% power to detect a difference of 7% in CCT, given a standard deviation of 7%.^{10,11}

Participants

This study involved 38 individuals with hyperosmolar tears and 10 age-similar controls with normo-osmolar tears, recruited from the University of Melbourne.

The inclusion criteria for the hyperosmolar tear group involved the presence of clinically significant dry eye symptoms²³ (ocular surface disease index [OSDI] score: 18–65) and tear hyperosmolarity²⁴ (≥ 316 mOsmol/L in at least one eye).²⁵ Eligibility criteria for the control (normo-osmolar) group were consistent with those proposed by Miller and colleagues²⁶ for symptoms (OSDI < 13) and by Lemp and colleagues²⁷ for tear osmolarity (< 308 mOsmol/L).

Exclusion criteria included: contact lens wear, anterior segment surgery, history of ocular disease (other than DED), active ocular allergy or infection, pregnancy or lactation, topical medications (other than ocular lubricants), punctal plug placement, or ocular trauma within 6 months of enrollment.

Potential participants underwent a comprehensive ophthalmic examination involving, in sequential order: symptom assessment (OSDI; Allergan Inc., Irvine, CA), tear osmolarity measurement, anterior-segment OCT, full slit-lamp examination (including sodium fluorescein [NaFl] tear break-up time [TBUT], corneal NaFl staining and conjunctival lissamine green [LG] staining), and Schirmer testing. All procedures were completed by the same clinician, in the same clinical environment, which was maintained at a temperature of $22 \pm 2^\circ\text{C}$ and humidity of $55 \pm 5\%$; participant examinations were undertaken between 10 AM and 3 PM, to minimize the potential influence of diurnal variations.

Tear Osmolarity

Tear osmolarity was assessed bilaterally using the TearLab system (TearLab Corp., San Diego, CA). The instrument was calibrated daily in accordance

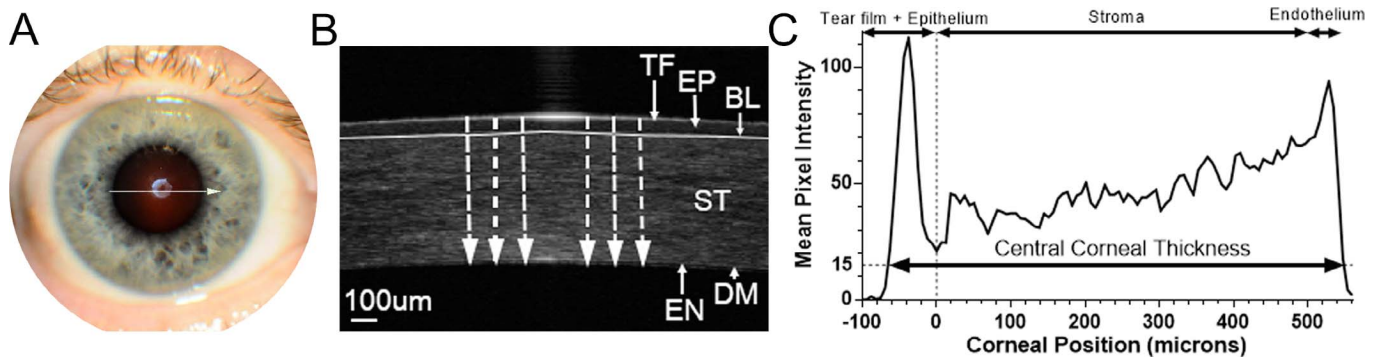


Figure 1. (A) An en face corneal image showing the location and direction of the 6.0-mm OCT B-scan captured through the corneal apex. (B) A representative averaged OCT image of the central 1.7 mm of the cornea. For each averaged OCT, Bowman's membrane was demarcated with a *white line* and the pixel intensity profile was measured for three vertical cross-sections, positioned approximately 100 μm apart (*dashed vertical white arrows*) as shown. Following alignment to Bowman's membrane (as the nominated 'zero' position for corneal depth), an average reflectivity profile was plotted. (C) A representative reflectivity profile, being the average of 18 scans (3 averaged OCT images \times 6 vertical cross-sections) normalized to mean background pixel intensity. The tear film and epithelium are represented by negative corneal location values, while the stroma and endothelium are represented by positive values. CCT was calculated as the distance between the two points with a threshold pixel intensity of 15 units, chosen to exclude background noise. TF, tear film; EP, corneal epithelium; BL, Bowman's layer; ST, corneal stroma; DM, Descemet's membrane; EN, corneal endothelium.

with manufacturer guidelines. Participants were instructed not to instill any eye drops 2 hours prior to testing. Room temperature was maintained at $22 \pm 2^\circ\text{C}$.²⁸

Tear Break-Up Time

TBUT was measured using NaFl-impregnated Dry Eye Tests (DET; Nomax Inc., St. Louis, MO) and diffuse blue illumination on a SL-D4 slit-lamp biomicroscope (Topcon Corporation, Tokyo, Japan) with $\times 10$ magnification and a Boston Wratten-12 yellow barrier filter (Bausch and Lomb, Rochester, NY). TBUT was recorded as the average of three consecutive readings measured using a stopwatch.

Ocular Surface Staining

Corneal and conjunctival staining assessment was performed using the method described by Bron and colleagues,²⁹ with NaFl for corneal staining and LG (Green Flo; HUB Pharmaceuticals, Rancho Cucamonga, CA) for conjunctival (nasal and temporal) staining. Staining was graded in 0.1 increments using the five-point Oxford grading scale.²⁹

Schirmer Test

Tear production was measured in a dimly lit room. Four minutes after instilling topical anesthetic (0.5% proxymetacaine hydrochloride; Alcon Laboratories, French Forest, NSW, Australia), a Schirmer strip

(Mark Blu; Optitech eyecare, Allahabad, India) was placed in the inferior lid margin and the participant closed their eyes. The strip was removed after 5 minutes; the amount of wetting was recorded (mm).

Anterior-Segment OCT

A Fourier-domain (FD) OCT (3D-OCT; Topcon Corporation) with an axial resolution of approximately $7 \mu\text{m}$ was used to capture three scans of 6-mm length through the central cornea. Participants were instructed to place their forehead and chin in the headrest, such that the OCT position and movement could be controlled in the x , y and z planes. Participants were positioned to ensure that all of the OCT images were captured through the corneal apex (Fig. 1A), defined as the position where specular reflection was evident. Each image was captured approximately 1 second after the participant was instructed to gently blink twice. The three OCT images, each hereby referred to as an 'averaged OCT' image, were extracted with each averaged OCT image being the mean of eight, 6-mm B-scans derived using the Topcon OCT software (Fig. 1B). These three averaged OCT images were used to quantify tear-epithelial interface reflectivity, corneal reflectivity, and CCT measurements. Although raw OCT reflectivity data is logarithmic in nature, normalized units (log over log) are reported in this study.

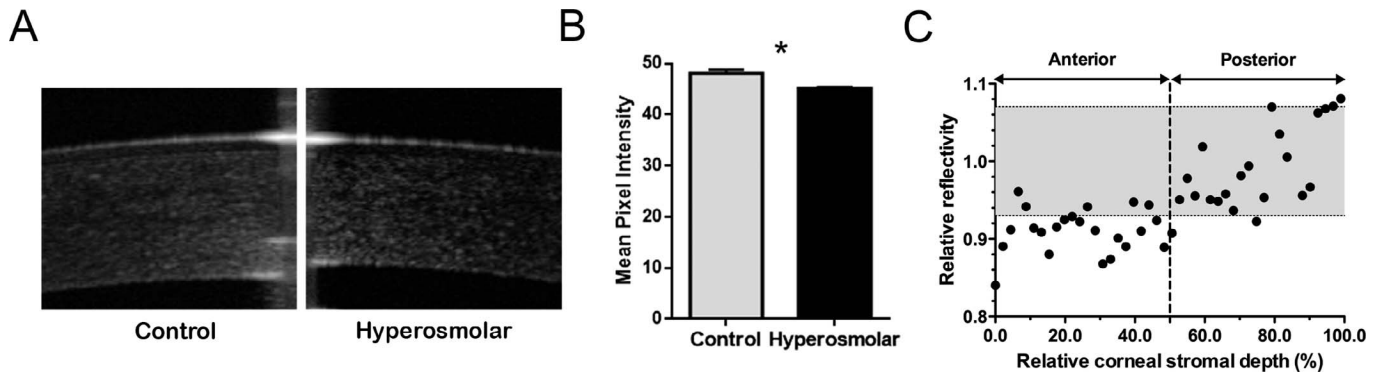


Figure 2. (A) Representative OCT B-scan images from the corneal apex of a control (normo-osmolar) participant (*left*) and an individual with hyperosmolar tears (*right*) that have been artificially juxtaposed, to highlight the reduction in CCT and decrease in anterior stromal reflectivity associated with tear hyperosmolarity. (B) Mean corneal stromal reflectivity was lower in hyperosmolar eyes relative to controls ($P < 0.05$). (C) Plot showing mean corneal stromal reflectivity in hyperosmolar eyes relative to controls; ‘relative reflectivity’ is defined as the hyperosmolar pixel intensity divided by the control pixel intensity across the relative stromal depth (%). The ‘relative reflectivity’ of the anterior corneal stroma is reduced in eyes with hyperosmolar tears. The *gray shaded area* represents the 95% confidence interval for corneal reflectivity in control (normo-osmolar) eyes. *Asterisks* show statistically significant differences between groups; $*P < 0.05$.

Image Analyses

Tear-Epithelial Interface Reflectivity and Corneal Reflectivity

Bowman’s layer, visible on the OCT scan as the dark band immediately beneath the highly reflective epithelial-tear interface, was manually demarcated using a white line on each of the averaged OCT images (Fig. 1B). For each averaged OCT image, the pixel intensity profile (measured in grayscale units; range, 0–255) of six vertically oriented corneal cross-sections were analyzed relative to the mean background pixel intensity using Matlab (vR2012a; Mathworks, Natick, MA). The ‘background noise’ was determined by sampling a horizontal line of pixels approximately 600 μm in length, at a position 10 microns down from the upper left corner of each OCT image.

Three cross-sections, separated by approximately 100 μm , were positioned either side of the corneal apex; interference from the zone of specular reflection was avoided (Fig. 1B). Reflectivity profiles were produced for each cross-section by plotting pixel intensity as a function of location. The 18 resultant reflectivity profiles (3 averaged OCT images \times 6 vertical cross-sections) were aligned relative to the demarcated Bowman’s layer (corneal position = 0, on the x axis). As such, regions to the left and right of this point represent the corneal epithelium + tear film (negative values) and stroma + endothelium (positive values), respectively. The artificially generated Bowman’s layer reference peak was replaced with a trough in each corneal reflectivity profile by substituting the

average of the pixel intensities immediately either side of this reference pixel in place of its nominal value of 255 (white) grayscale units.

The aligned profiles were averaged to produce a single profile, representing mean central corneal reflectivity for each eye. A representative averaged OCT image and average reflectivity profile is shown in Figures 1B and 1C, respectively. Central corneal reflectivity was calculated as the mean pixel intensity across the full CCT (Fig. 1C). Peak tear-epithelial reflectivity was defined as the average of the three adjacent pixels with the highest mean pixel intensity (i.e., first positive peak in Fig. 1C). Corneal stromal reflectivity was assessed in two components, being the mean pixel intensity averaged across the anterior and posterior halves of the corneal stroma (Fig. 1C). The ‘relative reflectivity’ of the corneal stroma (Fig. 2C), was calculated as the ratio of the mean corneal stromal reflectivity of hyperosmolar eyes ($n = 38$) relative to the mean corneal stromal reflectivity of normo-osmolar eyes ($n = 10$) across relative stromal depth (0.0–100.0%).

Central Corneal Thickness

CCT was measured as the longitudinal distance between the anterior and posterior corneal surface, as defined by the two points with a threshold pixel intensity of 15 grayscale units (Fig. 1C), as previously described.¹⁵ The criterion for the start and end of the corneal profile was chosen to exceed background noise (i.e., maximum background noise was 15.0 grayscale units).

Table. Study Participant Characteristics

	Control (Tear Normo-Osmolar) (<i>n</i> = 10)	Tear Hyperosmolar (<i>n</i> = 38)	<i>P</i> Value
Age, years	43.2 ± 6.0	42.8 ± 2.4	0.95
Female	50%	68%	0.02*
OSDI (/100)	7.1 ± 1.8	34.6 ± 2.1	< 0.0001***
Tear osmolarity, mOsmol/L	300.8 ± 1.7	327.6 ± 2.8	< 0.0001***
Corneal fluorescein staining (score /5.0)	0.4 ± 0.2	0.5 ± 0.1	0.78
Conjunctival lissamine green staining (score /10.0)	0.2 ± 0.1	0.7 ± 0.2	0.09
TBUT, s	11.3 ± 3.4	8.1 ± 0.8	0.39
Schirmer score, mm/5 minutes	10.6 ± 2.2	11.8 ± 1.5	0.66

Data are expressed as mean ± SEM. One participant with a tear osmolarity reading above the range measured by the TearLab osmometer (>400 mOsmol/L)⁵¹ was identified as an outlier using the Grubbs test and was removed from the analysis. Asterisks indicate statistically significant differences between groups.

* *P* < 0.05.

*** *P* < 0.001.

Statistical Analyses

The eye with higher tear osmolarity was defined as the ‘study eye’ and used for all analyses. GraphPad Prism (version 6.01; GraphPad Software, San Diego, CA) and SPSS (version 22.0; IBM Corp, Armonk, NY) were used to perform the statistical analyses. The normality of the data was assessed using the D’Agostino & Pearson omnibus test. Demographic and CCT data were analyzed using unpaired *t*-tests with Welch correction, the Wilcoxon rank sum test, or a χ^2 test as appropriate.

Tear-epithelial interface reflectivity and corneal reflectivity were compared between groups using a hierarchical design with main effect of group (hyperosmolar or control) and corneal location nested within subjects. The relationship between tear osmolarity and CCT was described with a two-line function with the transition allowed to float to minimize the sum-of-square error. For CCT, an exploratory analysis involving the subgrouping of hyperosmolar eyes by quartiles of tear hyperosmolarity was performed to assess for potential differential effects of mild (lower hyperosmolar quartile, Q1) versus severe (upper hyperosmolar quartile, Q4) elevations in tear tonicity relative to controls. The quartiles were defined based upon the method recommended by Joarder and Firozzaman,³⁰ who propose that a series of ordered sample observations should be evenly divided into four segments with the same number of observations in each segment. Given the sample size in this study (*n* = 38), the upper and lower quartiles

were defined first (Q1: *n* = 10 and Q4: *n* = 10), with the remaining 18 individuals evenly distributed into the second and third quartiles (Q2: *n* = 9 and Q3: *n* = 9).

A post-hoc power calculation for this comparison indicated 95% power to detect a statistically significant difference (alpha of 0.05) between the CCT of the upper quartile of hyperosmolar eyes (Q4) and control (normo-osmolar) eyes. Unless otherwise specified, data are expressed as mean ± standard error of the mean (SEM).

Results

Participant Characteristics

The Table summarizes the demographic and dry eye clinical characteristics of the study participants. OSDI scores (34.6 ± 2.1 vs. 7.1 ± 1.8, *P* < 0.0001), tear osmolarity (327.6 ± 2.8 vs. 300.8 ± 1.7, *P* < 0.0001), and proportion of females (68% vs. 50%, *P* = 0.02) were relatively higher in the tear hyperosmolar group. There was no difference between groups for age, Schirmer test, TBUT, corneal NaFl staining, or conjunctival LG staining.

Tear-Epithelial Interface Reflectivity and Corneal Reflectivity

Representative OCT scans are shown in Figure 2A. Peak tear-epithelial reflectivity relative to OCT background noise was comparably higher (4.8 ± 2.5%, *P* = 0.04) in the tear hyperosmolar group.

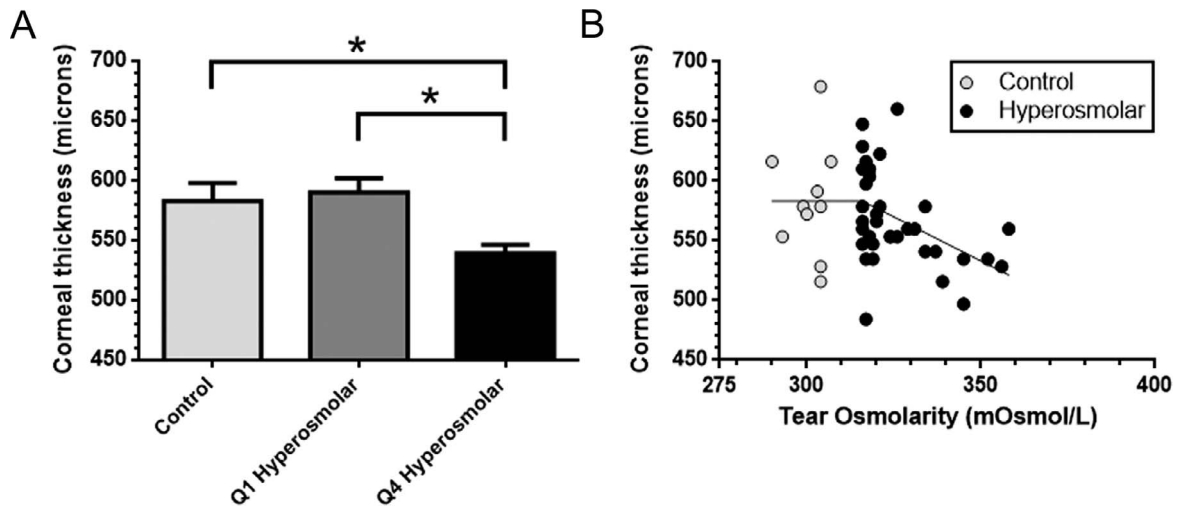


Figure 3. (A) CCT of control (normo-osmolar) eyes, eyes in the lower quartile (Q1) for tear osmolarity in the hyperosmolar group, and eyes in the upper quartile (Q4) for tear osmolarity in the hyperosmolar group. CCT was less in Q4 eyes compared with other groups. Asterisks show statistically significant differences between groups; $*P < 0.05$. (B) A two-line best fit of CCT data as a function of tear osmolarity shows a significant negative linear relationship between CCT for tear osmolarities of 316 mOsmol/L or greater ($R^2 = 0.17$, $P = 0.01$).

Central corneal reflectivity relative to OCT background noise was significantly less in hyperosmolar eyes (45.1 ± 0.3 vs. 48.1 ± 0.6 pixels, $P = 0.02$, Fig. 2B); difference was most pronounced in the anterior half of the corneal stroma where eyes with hyperosmolar tears had $4.7 \pm 1.9\%$ less corneal reflectivity (Fig. 2C, $P < 0.01$).

Central Corneal Thickness

Overall, there was no significant difference in CCT between study groups (hyperosmolar: $569.2 \pm 40.3 \mu\text{m}$, $n = 38$ versus normo-osmolar: $583.1 \pm 15.0 \mu\text{m}$, $n = 10$; $P > 0.05$). The CCT of the most severely hyperosmolar eyes ($539.1 \pm 7.4 \mu\text{m}$, $n = 10$), defined as those in the upper quartile (Q4) for osmolarity in the hyperosmolar group, was significantly thinner than both control eyes ($583.1 \pm 15.0 \mu\text{m}$, $P = 0.02$, $n = 10$) and eyes in the lower quartile (Q1) of the hyperosmolar group ($622.7 \pm 5.8 \mu\text{m}$, $P < 0.0001$, $n = 10$, Fig. 3A). There were no significant difference between normo-osmolar (control) eyes ($n = 10$) and the CCT of eyes in the second hyperosmolar quartile (Q2: $578.0 \pm 14.6 \mu\text{m}$, $n = 9$) or third hyperosmolar quartile (Q3: $554.2 \pm 4.9 \mu\text{m}$, $n = 9$). There was no relationship between CCT and tear osmolarity when osmolarity was less than 316 mOsmol/L (Fig. 3B). For tear osmolarity readings of 316 mOsmol/L or more, there was a significant, negative linear correlation ($R^2 = 0.17$, $P = 0.01$) with CCT. There was no significant difference in CCT between males and females in either the hyperosmolar or normo-

osmolar (control) groups ($P > 0.05$ for both comparisons).

Discussion

This study has used anterior segment OCT to investigate whether tear hyperosmolarity, being an ubiquitous feature of DED, affects central corneal reflectivity and/or thickness. We report, for the first time, that there are significant changes to CCT that relate to the degree of tear hyperosmolarity. Furthermore, we find both a relative increase in reflectivity of the tear film–epithelial interface and a reduction in corneal reflectivity in eyes with hyperosmolar tears. Specifically, eyes with hyperosmolar tears were found to have less relative central corneal reflectivity than control eyes, as measured from cross-sectional images captured with OCT using near infrared light; this effect was most pronounced in the anterior stroma.

Corneal transparency is known to depend upon the regular arrangement of collagen fibrils that encourage scattered light to undergo destructive interference, except in the direction of the incident beam.⁷ Changes to the spacing between the stromal collagen fibrils will affect the degree of destructive interference, thereby impacting upon corneal transparency.⁷ We propose that in DED, a subtle, hyperosmolarity-dependent alteration to corneal epithelial barrier function may promote the diffusion of water from the cornea into the tear film along osmotic gradients created by elevated tear osmolarity.

A chronic alteration to corneal dehydration would be predicted to impact upon the collagen fibril spacing, affecting the destructive interference of scattered light, which we find to be expressed clinically as reduced anterior stromal corneal reflectivity on OCT. Interestingly, our findings contrast with the corneal stromal hyperreflectivity response reported to occur following the induction of acute corneal thinning with a highly hypertonic solution in the rabbit cornea.³¹ This variance may relate to differences in the time course of changes to corneal hydration between these studies. In the investigation by Hosseini and colleagues,³¹ the dehydrating effect of an 100% hypertonic agent applied to the rabbit cornea was reported to involve an instantaneous and drastic corneal deswelling (i.e., up to 40% reduction in thickness within 10 minutes). In contrast, the effects of tear hyperosmolarity that we describe in this study reflect the outcome of a potentially long-term, low-grade osmotic challenge in a human clinical population; this scenario appears to yield a differential alteration to corneal ultrastructure, the significance of which is uncertain.

There is evidence that changes to corneal keratocytes can also influence the reflectivity properties of the cornea.^{32,33} In this respect, our findings for decreased stromal corneal reflectivity may indicate an altered number of corneal keratocytes and/or changes to keratocyte reflectivity within the anterior stroma in eyes having hyperosmolar tears. Interestingly, our finding of a hyporeflexivity response in the anterior corneal stroma contrasts with findings reported in more severe expressions of DED quantified using *in vivo* confocal microscopy. Sjögren's syndrome dry eye has been associated with hyperreflective changes in the corneal stroma that have been attributed to abnormal keratocyte activation.³² This increase in the density of hyperreflective keratocytes is similar to that described in Graves' disease, being another chronic autoimmune disorder that is characterized by systemic inflammation.³² As our study population consisted of individuals with mild to moderate DED, and not those with severe autoimmune forms of dry eye, it is possible that the findings reflect differential changes to corneal stromal architecture that are dependent upon the severity and etiology of the dry eye. A further consideration is that our study adopted OCT imaging, and involved quantifying corneal reflectivity using cross-sectional images of the cornea, in contrast to earlier studies that quantified changes to reflectivity used *en face* images

from confocal microscopy; this difference in methodology may also contribute to these findings.

Another noteworthy finding of this study is that the peak reflectivity of the tear-epithelial interface relative to OCT background reflectivity was relatively higher under conditions of hyperosmolarity. Experimental evidence has shown that while there is a correlation between refractometry and the osmolality of aqueous sodium chloride solution, this effect does not apply to human tears.³⁴ Rather, tear refractive index is linked more closely to composition, being moderately well correlated with tear lactoferrin levels.³⁴ These findings suggest that tear hyperosmolarity may be associated with significant changes to the tear proteome. Indeed, altered levels of tear proteins have been documented in heterogeneous clinical populations of dry eye patients.^{35–39}

In DED, decreased aqueous secretion and/or excessive tear evaporation results in reduced tear volume and increased tear osmolarity.⁴⁰ Based upon meta-analysis, a tear osmolarity value of 316 mOsmol/L has been proposed to be a sensitive diagnostic threshold for clinically significant DED.²⁴ Our data, which show a negative correlation between CCT and hyperosmolarity, suggest that tear osmolarity readings greater than 316 mOsmol/L disrupt the normal homeostatic osmotic gradient that exists between the cornea and tear film. This disruption likely contributes to the observed lower CCT, through increased fluid outflow from the corneal stroma into the hypertonic tear film. Clinical evidence describing an association between tear osmolarity and corneal thickness in humans with healthy tears is in support of this concept. Niimi and colleagues¹⁰ have shown that physiological, diurnal fluctuations in tear osmolarity correlate with changes to CCT of approximately 3.5% quantified using anterior-segment OCT. Furthermore, application of highly hypertonic agents to the ocular surface reduces corneal thickness by up to 30% in experimental animal models.^{9,41} Indeed, this rationale is applied in the therapeutic management of patients with severe corneal edema, such as bullous keratopathy, to reduce stromal swelling and improve visual acuity.⁴²

Because DED is more prevalent in females, we acknowledge that while there was a greater percentage of females in the tear hyperosmolar group, we consider the hyperosmolar group to be a representative sample of DED patients.⁴³ In addition, this finding is unlikely to affect the validity of CCT measurements given that CCT was found to not be significantly influenced by sex in this study or in a

previous investigation.⁴⁴ An acknowledged limitation of this study is that CCT measurements could not be automatically derived from the OCT device used, but instead were calculated from OCT images with the requirement for user input. To minimize the potential for operator error and/or bias, a robust, objective method of digital image analysis was adopted for this calculation, as previously reported.¹⁵ Our adoption of a custom threshold criterion for CCT calculations may also affect the direct comparability of absolute thickness measures relative to studies adopting different methods.

Our finding for reduced CCT in eyes with higher hyperosmolar tears has clinical implications for the measurement of intraocular pressure with applanation tonometry. Meta-analysis has shown that a 10% change in CCT alters the measured intraocular pressure by 3.4 ± 0.9 mm Hg.⁴⁵ Therefore, corneal thinning in severe DED may affect intraocular pressure readings, which can have implications for the diagnosis and monitoring of glaucoma.

The demonstrated capacity for OCT to detect subtle microstructural changes within the cornea and tear film provides a rationale to further investigate its application as a noninvasive diagnostic tool for ocular surface disease. Many of the tests in standard clinical use are relatively invasive⁴⁶ and demonstrate relative poor sensitivity and specificity for diagnosing DED.⁴⁷ While tear osmolarity assessment is regarded as a sensitive diagnostic test,⁴⁸ the ongoing cost of consumables and the requirement for daily calibration represent potential barriers to its widespread adoption.^{28,49} Similar to a recently defined novel clinical measure of tear stability,⁵⁰ OCT imaging is noninvasive and enables rapid image acquisition. Furthermore, we have shown the capacity for OCT to detect subtle, localized changes to tear film reflectivity, corneal reflectivity, and corneal thickness. The method we describe in this study to quantify changes to corneal reflectivity profiles could be applied to monitor microstructural changes in other anterior segment conditions affecting corneal transparency, including corneal infection, corneal scar regression, wound healing, and degenerative conditions, such as keratoconus or endothelial dystrophies. Studies investigating these additional potential applications are warranted.

This study demonstrates the application of anterior-segment FD-OCT to noninvasively assess the thickness and optical properties of the cornea and reflectivity properties of the tear film. We report relatively decreased CCT, reduced corneal reflectivity,

and heightened tear-epithelial reflectivity in individuals with hyperosmolar tears. Further studies on larger samples of participants with varying degrees of DED are necessary to examine the diagnostic potential of these new OCT-derived parameters.

Acknowledgments

Supported by a Rebecca L Cooper Medical Research Foundation Grant (LED). The funding organization had no role in the design or conduct of this research.

Disclosure: **L.A. Deinema**, None; **A.J. Vingrys**, None; **H.R. Chinnery**, None; **L.E. Downie**, None

References

1. Lemp M, Baudouin C, Baum J, et al. The definition and classification of dry eye disease: report of the Definition and Classification Subcommittee of the International Dry Eye Workshop (2007). *Ocul Surf*. 2007;5:75–92.
2. Ding J, Sullivan DA. Aging and dry eye disease. *Exp Gerontol*. 2012;47:483–490.
3. Nichols KK, Foulks GN, Bron AJ, et al. The international workshop on meibomian gland dysfunction: executive summary. *Invest Ophthalmol Vis Sci*. 2011;52:1922–1929.
4. Knop E, Knop N, Millar T, Obata H, Sullivan DA. The International Workshop on Meibomian Gland Dysfunction: report of the subcommittee on anatomy, physiology, and pathophysiology of the meibomian gland. *Invest Ophthalmol Vis Sci*. 2011;52:1938–1978.
5. Luo L, Li D-Q, Pflugfelder SC. Hyperosmolarity-induced apoptosis in human corneal epithelial cells is mediated by cytochrome c and MAPK pathways. *Cornea*. 2007;26:452–460.
6. De Paiva CS, Corrales RM, Villarreal AL, et al. Apical corneal barrier disruption in experimental murine dry eye is abrogated by methylprednisolone and doxycycline. *Ocul Surf*. 2006;2847:2856.
7. Maurice DM. The structure and transparency of the cornea. *J Physiol*. 1957;136:263–286.
8. Edelhauser HF. The balance between corneal transparency and edema: the Proctor Lecture. *Invest Ophthalmol Vis Sci*. 2006;47:1754–1767.
9. Hosseini K, Kholodnykh AI, Petrova IY, Esenaliyev RO, Hendrikse F, Motamedi M. Monitoring

- of rabbit cornea response to dehydration stress by optical coherence tomography. *Invest Ophthalmol Vis Sci.* 2004;45:2555–2562.
10. Niimi J, Tan B, Chang J, et al. Diurnal pattern of tear osmolarity and its relationship to corneal thickness and deswelling. *Cornea.* 2013;32:1305–1310.
 11. Liu Z, Pflugfelder SC. Corneal thickness is reduced in dry eye. *Cornea.* 1999;18:403–407.
 12. Kheirkhah A, Saboo US, Abud TB, et al. Reduced corneal endothelial cell density in patients with dry eye disease. *Am J Ophthalmol.* 2015;159:1022–1026, e1022.
 13. Adhikary G, Sun Y, Pearlman E. C-Jun NH2 terminal kinase (JNK) is an essential mediator of Toll-like receptor 2-induced corneal inflammation. *J Leuk Biol.* 2008;83:991–997.
 14. Johnson AC, Heinzl FP, Diaconu E, et al. Activation of toll-like receptor (TLR) 2, TLR4, and TLR9 in the mammalian cornea induces MyD88-dependent corneal inflammation. *Invest Ophthalmol Vis Sci.* 2005;46:589–595.
 15. Downie LE, Stainer MJ, Chinnery HR. Monitoring of strain-dependent responsiveness to TLR Activation in the mouse anterior segment using SD-OCT. *Invest Ophthalmol Vis Sci.* 2014;55:8189–8199.
 16. Izatt JA, Hee MR, Swanson EA, et al. Micrometer-scale resolution imaging of the anterior eye in vivo with optical coherence tomography. *Arch Ophthalmol.* 1994;112:1584–1589.
 17. Bechmann M, Thiel MJ, Neubauer AS, et al. Central corneal thickness measurement with a retinal optical coherence tomography device versus standard ultrasonic pachymetry. *Cornea.* 2001;20:50–54.
 18. Muscat S, McKay N, Parks S, Kemp E, Keating D. Repeatability and reproducibility of corneal thickness measurements by optical coherence tomography. *Invest Ophthalmol Vis Sci.* 2002;43:1791–1795.
 19. Hindman HB, Huxlin KR, Pantanelli SM, et al. Post-DSAEK optical changes: a comprehensive prospective analysis on the role of ocular wavefront aberrations, haze, and corneal thickness. *Cornea.* 2013;32:1567–1577.
 20. Wirbelauer C, Scholz C, Häberle H, Laqua H, Pham DT. Corneal optical coherence tomography before and after phototherapeutic keratectomy for recurrent epithelial erosions. *J Cataract Refract Surg.* 2002;28:1629–1635.
 21. Wang J, Thomas J, Cox I. Corneal light backscatter measured by optical coherence tomography after LASIK. *J Refr Surg.* 2006;22:604–610.
 22. Schmidl D, Witkowska KJ, Kaya S, et al. The association between subjective and objective parameters for the assessment of dry-eye syndrome. *Invest Ophthalmol Vis Sci.* 2015;56:1467–1472.
 23. Schiffman RM, Christianson MD, Jacobsen G, Hirsch JD, Reis BL. Reliability and validity of the Ocular Surface Disease Index. *Arch Ophthalmol.* 2000;118:615–621.
 24. Tomlinson A, Khanal S, Ramaesh K, Diaper C, McFadyen A. Tear film osmolarity: determination of a referent for dry eye diagnosis. *Invest Ophthalmol Vis Sci.* 2006;47:4309–4315.
 25. Deinema LA, Vingrys AJ, Wong C-Y, Jackson DC, Chinnery HR, Downie LE. A randomized, double-masked, placebo-controlled clinical trial of two forms of omega-3 supplements for treating dry eye disease. *Ophthalmology.* 2017;124:43–52.
 26. Miller KL, Walt JG, Mink DR, et al. Minimal clinically important difference for the ocular surface disease index. *Arch Ophthalmol.* 2010;128:94–101.
 27. Lemp MA, Bron AJ, Baudouin C, et al. Tear osmolarity in the diagnosis and management of dry eye disease. *Am J Ophthalmol.* 2011;151:792–798.
 28. Downie LE, Vingrys AJ. Accuracy of laboratory assays in ophthalmic practice. *JAMA Ophthalmol.* 2015;133:1480.
 29. Bron AJ, Evans VE, Smith JA. Grading of corneal and conjunctival staining in the context of other dry eye tests. *Cornea.* 2003;22:640–650.
 30. Joarder A, Firozzaman M. Quartiles for discrete data. *Teaching Statistics.* 2001;23:86–89.
 31. Hosseini K, Kholodnykh AI, Petrova IY, Esenaliyev RO, Hendrikse F, Motamedi M. Monitoring of rabbit cornea response to dehydration stress by optical coherence tomography. *Invest Ophthalmol Vis Sci.* 2004;45:2555–2562.
 32. Miller-Pedersen T. Keratocyte reflectivity and corneal haze. *Exp Eye Res.* 2004;78:553–560.
 33. Alhatem A, Cavalcanti B, Hamrah P. In vivo confocal microscopy in dry eye disease and related conditions. *Semin Ophthalmol.* 2012;27:138–148.
 34. Craig JP. Refractive index and osmolality of human tears. *Optom Vis Sci.* 1995;72:718.
 35. Boehm N, Funke S, Wiegand M, Wehrwein N, Pfeiffer N, Grus FH. Alterations in the tear proteome of dry eye patients—a matter of the clinical phenotype. *Invest Ophthalmol Vis Sci.* 2013;54:2385–2392.

36. Grus FH, Podust VN, Bruns K, et al. SELDI-TOF-MS ProteinChip array profiling of tears from patients with dry eye. *Invest Ophthalmol Vis Sci.* 2005;46:863–876.
37. Ohashi Y, Ishida R, Kojima T, et al. Abnormal protein profiles in tears with dry eye syndrome. *Am J Ophthalmol.* 2003;136:291–299.
38. Zhou L, Beuerman RW, Chan CM, et al. Identification of tear fluid biomarkers in dry eye syndrome using iTRAQ quantitative proteomics. *J Proteome Res.* 2009;8:4889–4905.
39. Jackson D, Zeng W, Wong C, et al. Tear interferon-gamma as a biomarker for evaporative dry eye disease. *Invest Ophthalmol Vis Sci.* 2016;57:4824–4830.
40. Lemp MA, Foulks GN. The definition and classification of dry eye disease. *Ocul Surf.* 2007;5:75–92.
41. Inslar MS, Benefield DW, Ross VE. Topical hyperosmolar solutions in the reduction of corneal edema. *Eye Contact Lens.* 1987;13:149–151.
42. Knezovic I, Dekaris I, Gabric N, et al. Therapeutic efficacy of 5% NaCl hypertonic solution in patients with bullous keratopathy. *Coll Antropol.* 2006;30:405–408.
43. Maïssa C, Guillon M. Tear film dynamics and lipid layer characteristics—effect of age and gender. *Contact Lens Anterior Eye.* 2010;33:176–182.
44. Cho P, Lam C. Factors affecting the central corneal thickness of Hong Kong-Chinese. *Curr Eye Res.* 1999;18:368–374.
45. Doughty MJ, Zaman ML. Human corneal thickness and its impact on intraocular pressure measures. *Surv Ophthalmol.* 44:367–408.
46. Downie LE, Keller PR, Vingrys AJ. An evidence-based analysis of Australian optometrists' dry eye practices. *Optom Vis Sci.* 2013;90:1385–1395.
47. Downie LE, Keller PR. A pragmatic approach to dry eye diagnosis: evidence into practice. *Optom Vis Sci.* 2015;92:1189–1197.
48. Sullivan BD, Whitmer D, Nichols KK, et al. An objective approach to dry eye disease severity. *Invest Ophthalmol Vis Sci.* 2010;51:6125–6130.
49. Farris RL. Tear osmolarity—a new gold standard? In: DA, Sullivan ME, Stern Tsubota K, Dartt DA, RM, Sullivan Bromberg BB, eds. *Lacrimal Gland, Tear Film, and Dry Eye Syndromes.* New York: Springer; 1994:495–503.
50. Downie LE. Automated tear film surface quality breakup time as a novel clinical marker for tear hyperosmolarity in dry eye disease. *Invest Ophthalmol Vis Sci.* 2015;56:7260–7268.
51. TearLab Corporation. TearLab osmolarity system - clinical utility guide. San Diego, CA; 2012.



Minerva Access is the Institutional Repository of The University of Melbourne

Author/s:

Deinema, LA; Vingrys, AJ; Chinnery, HR; Downie, LE

Title:

Optical Coherence Tomography Reveals Changes to Corneal Reflectivity and Thickness in Individuals with Tear Hyperosmolarity

Date:

2017-05-01

Citation:

Deinema, L. A., Vingrys, A. J., Chinnery, H. R. & Downie, L. E. (2017). Optical Coherence Tomography Reveals Changes to Corneal Reflectivity and Thickness in Individuals with Tear Hyperosmolarity. TRANSLATIONAL VISION SCIENCE & TECHNOLOGY, 6 (3), <https://doi.org/10.1167/tvst.6.3.6>.

Persistent Link:

<http://hdl.handle.net/11343/212712>

File Description:

Published version

License:

CC BY-NC-ND